Oncogene (2007) 26, 4415–4427

www.nature.com/onc

ORIGINAL ARTICLE

Conditional expression of mutated K-*ras* accelerates intestinal tumorigenesis in *Msh2*-deficient mice

F Luo[1], DG Brooks[1], H Ye[1], R Hamoudi[1], G Poulogiannis[1], CE Patek[2], DJ Winton[3] and MJ Arends[1]

[1]*Department of Pathology, Addenbrooke's Hospital, University of Cambridge, Cambridge, UK;* [2]*Sir Alastair Currie Cancer Research UK Laboratory, Molecular Medicine Centre, The University of Edinburgh, Western General Hospital, Edinburgh, UK and* [3]*Department of Oncology, Cambridge Institute of Medical Research, Addenbrooke's Hospital Campus, University of Cambridge, Cambridge, UK*

K-*ras* mutation occurs in 40–50% of human colorectal adenomas and carcinomas, but its contribution to intestinal tumorigenesis *in vivo* is unclear. We developed K-ras^{V12} transgenic mice that were crossed with *Ah-Cre* mice to generate K-ras^{V12}/*Cre* mice, which showed β-naphthoflavone-induction of *Cre*-mediated *LoxP* recombination that activated intestinal expression of K-ras^{V12} 4A and 4B transcripts and proteins. Only very occasional intestinal adenomas were observed in β-naphthoflavone-treated K-ras^{V12}/*Cre* mice aged up to 2 years, suggesting that mutated K-*ras* expression alone does not significantly initiate intestinal tumourigenesis. To investigate the effects of mutated K-*ras* on DNA mismatch repair (MMR)-deficient intestinal tumour formation, these mice were crossed with $Msh2^{-/-}$ mice to generate K-ras^{V12}/*Cre*/$Msh2^{-/-}$ offspring. After β-naphthoflavone treatment, K-ras^{V12}/*Cre*/$Msh2^{-/-}$ mice showed reduced average lifespan of 17.3±5.0 weeks from 26.9±6.8 (control $Msh2^{-/-}$ mice) ($P<0.01$). They demonstrated increased adenomas in the small intestine from 1.41 ($Msh2^{-/-}$ controls) to 7.75 per mouse (increased fivefold, $P<0.01$). In the large intestine, very few adenomas were found in $Msh2^{-/-}$ mice (0.13 per mouse) whereas K-ras^{V12}/*Cre*/$Msh2^{-/-}$ mice produced 2.70 adenomas per mouse (increased 20-fold, $P<0.01$). Over 80% adenomas from K-ras^{V12}/*Cre*/$Msh2^{-/-}$ mice showed transgene recombination with expression of K-ras^{V12} 4A and 4B transcripts and proteins. Sequencing of endogenous murine K-*ras* showed mutations in two out of 10 tumours examined from $Msh2^{-/-}$ mice, but no mutations in 17 tumours from K-ras^{V12}/*Cre*/$Msh2^{-/-}$ mice. Expression of K-ras^{V12} in tumours caused activation of the mitogen-activated protein kinase and Akt/protein kinase B signaling pathways, demonstrated by phosphorylation of p44MAPK, Akt and GSK3β, as well as transcriptional upregulation of *Pem*, *Tcl-1* and *Trap1a* genes (known targets of K-ras^{V12} expression in stem cells). Thus, mutated K-*ras* cooperates synergistically with MMR deficiency to accelerate intestinal tumorigenesis, particularly in the large intestine.
Oncogene (2007) **26,** 4415–4427; doi:10.1038/sj.onc.1210231; published online 5 February 2007

Keywords: K-*ras*; *Cre-LoxP*; intestine; tumour; mouse

Introduction

Colorectal tumour formation involves progression from normal epithelium to adenomas to carcinomas associated with multiple genetic and epigenetic alterations (Kinzler and Vogelstein, 1996). K-*ras* mutation occurs in 40–50% of human colorectal adenomas and carcinomas, but how oncogenic K-*ras* contributes to or modulates the processes of intestinal tumour formation *in vivo* is unclear (Barbacid, 1987). K-*ras* mutations may be found at all stages of colorectal pre-neoplastic and neoplastic lesions, including dysplastic aberrant crypt foci (microadenomas) (Shivapurkar *et al*., 1997) and hyperplastic polyps (Otori *et al*., 1997), as well as in apparently normal large intestinal epithelium taken from tumour-bearing colons (Morris *et al*., 1996; Yamada *et al*., 2005). K-*ras* mutations are associated with increased size and dysplasia in adenomas, suggesting that they may be permissive for growth disorder early in tumorigenesis (Malumbres and Barbacid, 2003). Mutation of the K-*ras* gene typically occurs at either codons 12 or 13 (or occasionally at codon 61), with the codon 12 glycine to valine substitution being the most aggressive mutation associated with poor prognosis (Andreyev *et al*., 2001). These mutations reduce or abolish the protein's intrinsic GTPase activity when complexed with GAPs, tending to lock K-Ras in a GTP bound conformation that is constitutively active (Barbacid, 1987). This mutational activation of *ras* has several effects on cells *in vitro* and *in vivo*, including the establishment of the transformed phenotype, anchorage-independent growth, focus formation, increased proliferation, tumorigenic potential, changes in differentiation and altered susceptibility to apoptosis

Correspondence: Dr MJ Arends, Department of Pathology, University of Cambridge, Box 235, Addenbrooke's Hospital, Hills Road, Cambridge, CB2 2Q, UK.
E-mail: mja40@cam.ac.uk
Received 18 January 2006; revised 13 October 2006; accepted 21 November 2006; published online 5 February 2007

(Spandidos and Wilkie, 1984; Arends *et al*., 1993, 1994; Brooks *et al*., 2001; James *et al*., 2003; Plowman *et al*., 2003, 2006a, b).

Inherited mutations in DNA mismatch repair (MMR) genes in humans are directly involved in the aetiology of hereditary non-polyposis colorectal cancer syndrome (HNPCC), and confer pre-disposition to colorectal and other tumours (Arends and Frayling, 2004). The primary function of the MMR system is to eliminate base-to-base mismatches and insertion–deletion (in–del) loops that arise during DNA replication. Base-to-base mismatches involve the inappropriate substitution of one base for another and typically occur within sections of non-repetitive DNA, whereas in–del loops usually involve the loss or gain of repetitive sequence units such as (A)n, (CA)n repeats or other microsatellites, giving rise to microsatellite instability in MMR-defective cells. In mammals, mismatch or in–del loop recognition is attributed to heterodimeric protein complexes of MutS homologues, MSH2-MSH3 and MSH2-MSH6, which interact with a heterodimer of two MutL homologues, MLH1-PMS2 and MLH1-PMS1 (Toft and Arends, 1998; Jiricny and Nystrom-Lahti, 2000; Frayling *et al*., 2005). As loss of MSH2 inactivates the activity of mismatch and in–del loop recognition heterodimers, MSH2 deficiency causes strong cancer predisposition in both mice and humans (de Wind *et al*., 1995, 1998; Reitmair *et al*., 1995, 1996; Toft *et al*., 1998, 1999, 2002).

To clarify the role of expression of mutated K-*ras* in intestinal tumour development and progression *in vivo*, we developed and characterized mice with a transgene allowing inducible intestinal crypt epithelial stem cell expression of K-*ras*^{V12} via a *Cre*/*LoxP* system. Only very occasional intestinal tumours were found in these mice over 1–2 years. Therefore, we crossed these mice with *Msh2*-deficient mice to examine the effects of mutated K-*ras* on progression of MMR-deficient intestinal tumorigenesis. We found that intestinal expression of K-*ras*^{V12} in *Msh2*-null mice led to reduced survival and a marked increase in both small and large intestinal tumour (LIT) multiplicity, with the greater effect found on tumours of the colon and rectum, as in humans.

Results

Generation of conditional transgenic K-ras^{V12} *mice*

The conditional K-*ras*^{V12} expression transgene is based on the human K-*ras*^{V12} 'minigene' sequence (with an activating mutation at codon 12 substituting valine for glycine) inserted into a vector with a floxed *Neo*-containing 'STOP' cassette separating the K-*ras*^{V12} 'minigene' from the cytomegalovirus (*CMV*) promoter upstream. An internal ribosomal entry site (*IRES*) and enhanced green fluorescent protein (*EGFP*) sequence were inserted downstream to generate the final transgene construct called K-*ras*^{V12} shown in Figure 1. The K-*ras*^{V12} 'minigene' possesses intronic sequences allowing expression of both K-*ras* 4A and 4B transcript isoforms (Figure 1). The structure of the construct was confirmed

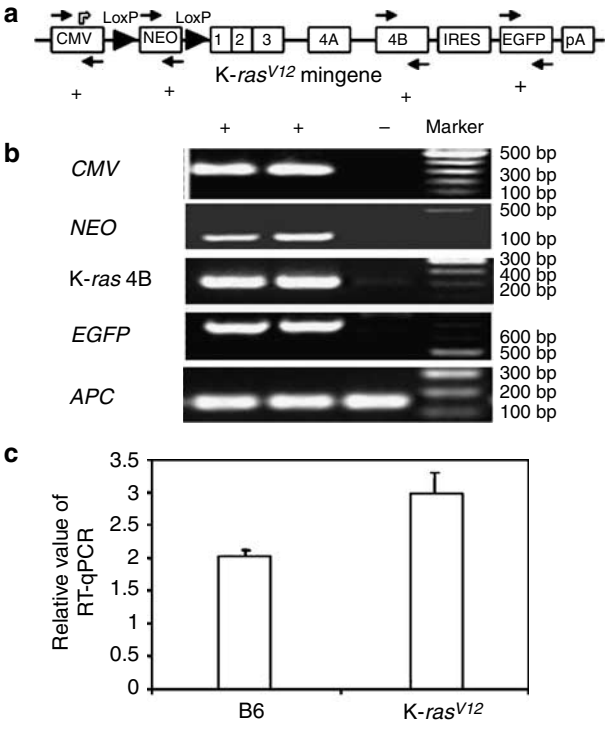

Figure 1 Schematic representation of the K-*ras*^{V12} transgene construct with the PCR-based genotyping assays and copy number assay. (**a**) Structure of the K-*ras*^{V12} transgene. *CMV*, cytomegalovirus immediate early promoter; *NEO*, *Neo*-containing 'STOP' cassette; 1, 2, 3, 4A and 4B, exons 1, 2, 3, 4A and 4B of the K-*ras*^{V12} gene; *IRES*, encephalomyocarditis virus internal ribosome entry site; *EGFP*, EGFP gene; pA, polyadenylation signal; ▶, 34 bp *LoxP* sites. Position and orientation of the PCR primers used for the genotyping analyses are depicted by arrows. (**b**) Typical results of genotyping PCR assays from offspring of transgenic mice and B6 mice. PCR amplification of an *APC* gene fragment was used to control the quality of genomic DNA samples. + represents mouse tail DNA from mice positive for the K-*ras*^{V12} transgene; – represents mouse tail DNA from B6 mice negative for the K-*ras*^{V12} transgene construct. (**c**) Bar chart of relative copy numbers by RT–qPCR of K-*ras* exon 3 sequences (human and mouse) which were 2.01 ± 0.11 in B6 control mice ($n = 6$) and 2.99 ± 0.34 in K-*ras*^{V12} mice ($n = 6$).

by restriction enzyme digestion and DNA sequencing (data not shown). In order to confirm the correct functioning of the construct *in vitro*, the expression vector was transfected into HM1 murine embryonic stem (ES) cells, which were transiently transfected with a plasmid expressing *Cre*. Subsequent real time–polymerase chain reaction (RT–PCR) analysis showed expression of mutated human K-*ras* transcripts in these ES cells (data not shown). The K-*ras*^{V12} transgene construct was linearized by *Bam*HI, purified and microinjected into fertilized *FVB*/*N* mouse oocytes. Two K-*ras*^{V12} founder mice were generated; one of which died and the other founder (shown to be K-*ras*^{V12} transgene positive) was crossed with B6 mice.

Analysis of the transgene copy number in K-ras^{V12} *transgenic mice*

The surviving founder K-*ras*^{V12} transgene positive mouse (F0) was crossed with B6 mice, and after three

generations (F1, F2 and F3), a total of 106 offspring were obtained, the number of B6 offspring mice was 54 (26 male and 28 female) and the number of K-*ras*^{V12} positive offspring mice (identified by PCR assays for presence of *CMV* promoter, human K-*ras*, *Neo* and *EGFP* gene) was 52 (27 male and 25 female) (Figure 1). Thus, the ratio of B6 to K-*ras*^{V12} offspring mice and the ratio of male to female offspring mice were both close to 1:1 (in a Mendelian ratio). The results suggested that the K-*ras*^{V12} transgene construct was integrated into a single site of an autosomal chromosome in the transgenic line.

The exon 3 DNA sequences of human and mouse K-*ras* genes are highly homologous with a DNA sequence difference of only two base pairs. A pair of PCR primers was designed to bind equally to both human and murine K-*ras* exon 3 DNA sequences and quantitative polymerase chain reaction (RT–qPCR) analysis showed the relative value of K-*ras* exon 3 copy number in B6 control mice was 2.01 ± 0.11 (mean $\pm$ s.d.; $n = 6$) and that in K-*ras*^{V12} transgenic mice was 2.99 ± 0.34 ($n = 6$), indicating that B6 control mice have two endogenous copies of K-*ras*, but K-*ras*^{V12} transgenic mice have three copies, including the two normal endogenous murine K-*ras* genes and one extra copy of the K-*ras*^{V12} transgene construct integrated into the genome of the mice (Figure 1).

Conditional expression of Cre and K-ras^{V12} *in the intestines*

K-*ras*^{V12} transgene positive mice were crossed with *Ah-Cre* mice that are capable of transient expression of Cre recombinase protein in the epithelial stem cells of the intestinal crypts following β-naphthoflavone (β-NF) intraperitoneal injection (Ireland *et al*., 2004). This generated offspring mice positive for both conditional K-*ras*^{V12} and *Ah-Cre* transgenes, confirmed by PCR-based genotyping assays. The test group of 28 mice (positive for both K-*ras*^{V12} and *Cre* transgenes) were treated with β-NF (16 mg/kg per day for 6 days) to induce transient expression of Cre recombinase protein in intestinal epithelium. Using the PCR assay to detect recombination occurring at the two *LoxP* sites (flanking the 'STOP' cassette) which amplifies the DNA fragment between the two primers (one situated in the *CMV* promoter and the other situated in K-*ras*^{V12} exon 3), a $\sim$500 bp fragment (indicating *LoxP* recombination) was amplified from genomic DNA extracted from both large and small intestines, caecum, stomach and also from liver, lung and spleen (Figure 2). This showed that Cre-mediated recombination at the two *LoxP* sites had occurred to excise the large $\sim$2 kb 'STOP' cassette containing the *Neo* gene, bringing together the *CMV* promoter sequence and the K-*ras*^{V12} sequence. This was confirmed by DNA sequencing of this PCR product which showed that the *Neo*-containing 'STOP' cassette had been deleted between the two *Not*I sites, leaving only one *LoxP* site between the *CMV* promoter and adjacent K-*ras* sequence (Figure 2). The sequencing data also confirmed the presence of valine at codon 12 (substituted for glycine) (Figure 2). RT–PCR analysis confirmed the expression of human K-*ras* transcripts in different tissues of K-*ras*^{V12}/*Cre* transgenic mice (but not in K-*ras*^{V12} transgenic mice that were negative for *Ah-Cre*) after β-NF treatment, including expression of both K-*ras*^{V12} 4A and 4B transcripts in all parts of the gastrointestinal tract (stomach, caecum, all parts of both small and large intestines) and also in liver, pancreas, kidney, lung and spleen, but not in heart or skin (Figure 3). Western blot analysis using anti-Cre antibody showed Cre protein expression in the small and large intestines 5–10 days after β-NF injection (Figure 3). Western blot analysis using specific anti-K-Ras^{V12} protein antibody showed mutant K-Ras protein expressed in the small and large intestines 1 week after β-NF injection in K-*ras*^{V12}/*Cre* transgenic mice (Figure 3). Anti-pan-K-Ras antibody showed some background expression of endogenous Ras in control mice (both B6 and Cre mice), but increased expression of Ras protein in the test group of K-*ras*^{V12}/*Cre* transgenic mice injected with β-NF (Figure 3).

Intestinal phenotypic changes in K-ras^{V12}/*Cre mice*

The test group of 28 K-*ras*^{V12}/*Cre* transgenic mice, aged 4–5 weeks, was treated with β-NF to activate Cre expression and K-*ras*^{V12} transgene recombination in the small and large intestines and was closely monitored for tumour development. Eight mice were killed after 1 year and 20 mice were monitored for nearly 2 years for signs of intestinal tumour development. During this period, only two intestinal adenomas were detected towards the end of the 2-year period (one in the large intestine and one in the small intestine) in two separate mice, compared with no intestinal tumours in the control B6 mice ($n = 16$) or *Cre*-only mice ($n = 29$) (treated in the same way) over the same 2-year period. No tumours were observed in other tissues in test or control mice. Histological examination of the small and large intestines from the K-*ras*^{V12}/*Cre* transgenic mice showed no evidence of proliferative or differentiation abnormalities (no hyperplastic polyps, no increase in size of the intestinal crypts or villi and no increase in frequency of mitotic figures). The results suggest that conditional expression in the intestines of mutated K-*ras* does not act as an initiating event in intestinal tumorigenesis *in vivo* to any significant extent.

Survival and intestinal tumour incidence in K-ras^{V12}/*Cre*/*Msh2*$^{-/-}$ *mice*

To assess the effects of conditional intestinal expression of K-*ras*^{V12} on MMR-deficient intestinal tumorigenesis, we crossed K-*ras*^{V12} mice with *Msh2*$^{-/-}$ mice to derive K-*ras*^{V12}/*Msh2*$^{+/-}$ mice, which were back-crossed with *Msh2*$^{-/-}$ mice to derive K-*ras*^{V12}/*Msh2*$^{-/-}$ mice. These were crossed with *Msh2*$^{-/-}$/*Cre* mice to generate a cohort of 25 K-*ras*^{V12}/*Cre*/*Msh2*$^{-/-}$ test mice. Four to five weeks after birth, these test mice were injected with β-NF (16 mg/kg per day for 6 days). Owing to tumour development the average life span of the mice decreased to 17.3 ± 5.0 weeks (mean $\pm$ s.d. for the 25 β-NF-treated K-*ras*^{V12}/*Cre*/*Msh2*$^{-/-}$ test mice) from 26.9 ± 6.8 (for the

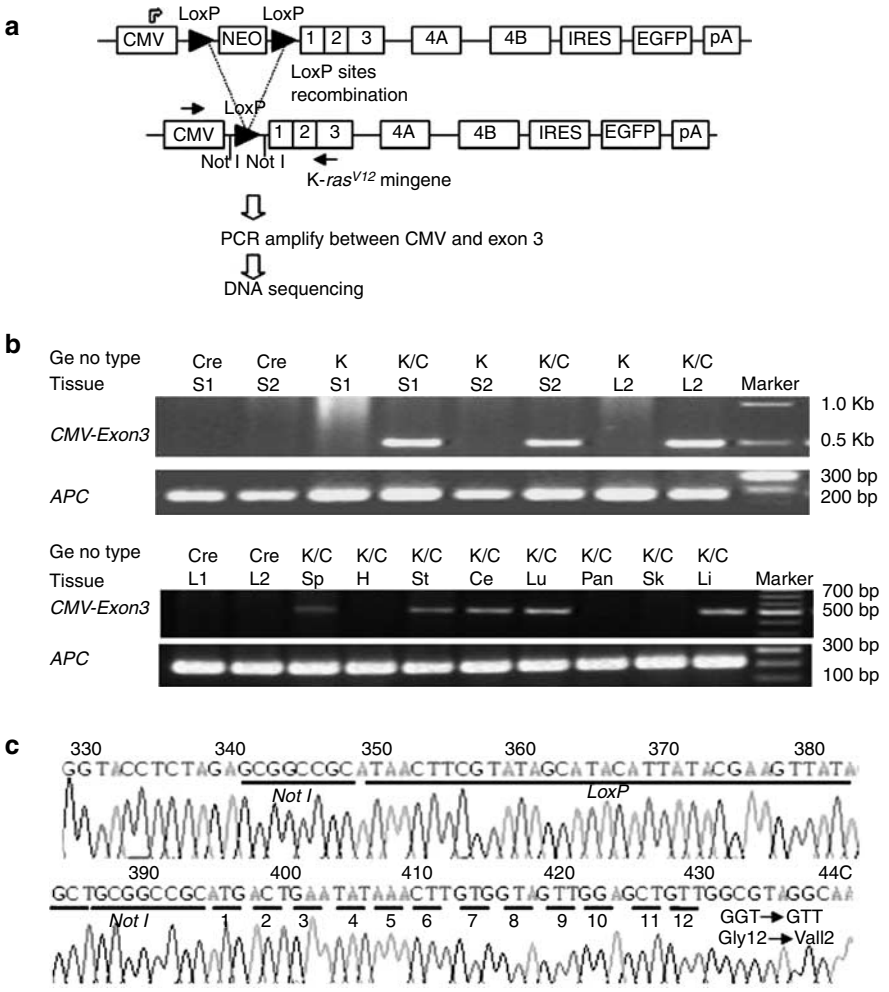

Figure 2 Conditional Cre-mediated recombination at the *LoxP* sites of the K-*ras*^{V12} transgene in various tissues. (**a**) Schematic representation of the K-*ras*^{V12} transgene construct showing Cre-mediated recombination at the two *LoxP* sites (▶) with excision of the *Neo*-containing 'STOP' cassette placing the K-*ras*^{V12} 'minigene' directly under the control of the *CMV* promoter to activate its expression. The position and orientation of the PCR primers in the *CMV* promoter and K-*ras* exon 3 are depicted by arrows. (**b**) Transgene recombination assay with PCR amplification of genomic DNA, using primers located in the *CMV* promoter and K-*ras*^{V12} exon 3, generated a ~500 bp fragment from recombined sequences in the small and large intestines and in stomach, caecum, liver, lung and spleen. Cre, *Ah-Cre* transgenic mice; K, K-*ras*^{V12} transgenic mice; K/C, K-*ras*^{V12}/*Cre* transgenic mice; S1, first half of small intestine nearest stomach; S2, second half of small intestine nearest caecum; L1, first half of large intestine nearest ileum; L2, second half of large intestine nearest anus; Sp, spleen; H, heart; St, stomach; Ce, Caecum; Pan; Pancreas; Sk, skin; Li, liver; Lu, lung. PCR amplification of an *APC* gene fragment was used to control the quality of genomic DNA samples. (**c**) DNA sequence data from one of the intestinal-derived ~500 bp amplified fragments, using primers located in the *CMV* promoter and K-*ras* exon 3, showing that the *Neo*-containing 'STOP' cassette has been deleted and there is only one *LoxP* site flanked by two *NotI* sites and that the K-*ras* codon 12 sequence is GTT (valine) and not the wild-type GGT (glycine) sequence.

25 β-NF-treated control mice that were *Msh2*$^{-/-}$, consisting of 18 *Msh2*$^{-/-}$ littermates and seven *Msh2*$^{-/-}$/*Cre* littermates) ($P<0.01$) (Figures 4 and 5). No sex differences in lifespan were observed for either group. None of the 25 β-NF-treated *Msh2*$^{-/-}$-control mice developed intestinal tumours before 5 months. However, after β-NF treatment, the K-*ras*^{V12}/*Cre*/*Msh2*$^{-/-}$ test mice showed intestinal tumours as early as 3.5 months and the number and location of tumours changed when comparing tumour development in *Msh2*$^{-/-}$ control mice with that in K-*ras*^{V12}/*Cre*/*Msh2*$^{-/-}$ test mice: duodenal tumours increased from 0.13 ± 0.46 to 1.06 ± 1.14 (8.15-fold increase, $P<0.01$); jejunal tumours from 1.05 ± 1.14 to 4.98 ± 1.97 (4.74-fold, $P<0.01$); ileal tumours from 0.23 ± 0.42 to 1.71 ± 1.40 (7.43-fold, $P<0.01$); proximal colonic tumours from 0.04 ± 0.21 to 1.18 ± 1.11 (29.5-fold, $P<0.01$) and distal colonic tumours from 0.09 ± 0.29 to 1.52 ± 1.54 (16.8-fold, $P<0.01$) (Figures 4 and 5). The total incidence of tumours in the small intestines and large intestines in β-NF-treated K-*ras*^{V12}/*Cre*/*Msh2*$^{-/-}$ mice was increased from 1.41 (*Msh2*$^{-/-}$ controls) to 7.75 per mouse in the small intestine (fivefold, $P<0.01$), and from 0.13 per mouse (*Msh2*$^{-/-}$ controls) to 2.70 adenomas per mouse (20-fold, $P<0.01$) in the large intestine. The intestinal adenomas in the test and control groups

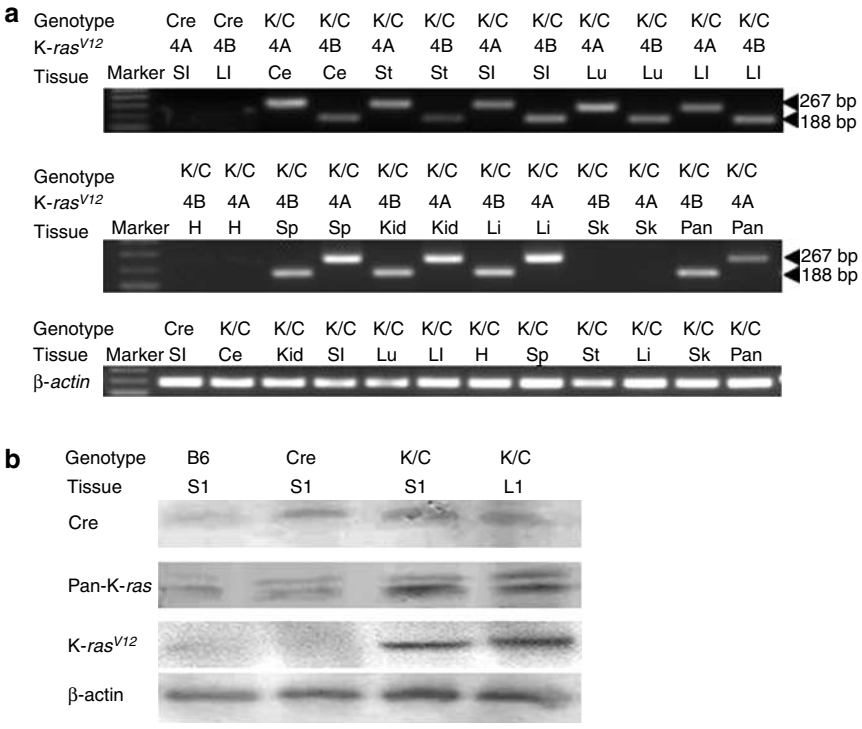

Figure 3 Analysis of expression of K-*ras*^{V12} RNA and protein and Cre protein in murine tissues. (**a**) RT–PCR analysis of the expression of K-*ras*^{V12} 4A and 4B transcript isoforms in different tissues of K-*ras*^{V12}/*Cre* transgenic mice, induced by 6 days of β-NF treatment and samples taken 10 days after completion of the β-NF treatment. Cre, K/C, L1, S1, Ce, St, H, Sp, Li, Sk, Pan, Lu as described in Figure 2; Kid, Kidney; 4A, 4A transcript of human K-*ras*^{V12}; 4B, 4B transcript of human K-*ras*^{V12}. Both K-*ras*^{V12} 4A and 4B transcripts are expressed in similar ratios in small and large intestines, stomach, caecum, liver, pancreas, kidney, lung and spleen, but not in skin or heart of β-NF-treated K-*ras*^{V12}/*Cre* transgenic mice. RT–PCR amplification of a β-actin transcript fragment was used to control the quality of RNA samples. (**b**) Western blot analysis of the expression of either Cre recombinase protein or K-Ras protein using anti-Cre antibody, anti-pan-K-*ras* antibody or anti-K-Ras^{V12} antibody in the intestines of K-*ras*^{V12}/*Cre* transgenic mice after β-NF treatment as above. Cre, K/C, L1, S1, as described above; B6, B6 control mice were also treated with β-NF.

did not differ in terms of the range of sizes observed, tumour stage (there were no invasive adenocarcinomas found) or degree of dysplasia (the adenomas all showed a similar appearance of moderate to severe dysplasia). No evidence of metastatic deposits was found in any of the tumour-bearing mice on examination of liver, lungs, peritoneal surfaces and other organs. None of the β-NF-treated *Cre*-only ($n=29$) or *Msh2*$^{+/-}$ ($n=16$) littermate control mice developed intestinal or other tumours within the same period of observation.

The incidence of thymic lymphomas was increased from 16% (4/25) for β-NF-treated *Msh2*$^{-/-}$-control mice to 44% (11/25) for β-NF-treated K-*ras*^{V12}/*Cre*/*Msh2*$^{-/-}$ test mice, and the size of thymic lymphomas also was increased from 2.16 ± 5.25 mm average ($\pm$s.d.) diameter (for *Msh2*$^{-/-}$-control mice) to 5.64 ± 7.62 mm for β-NF-treated K-*ras*^{V12}/*Cre*/*Msh2*$^{-/-}$ test mice ($P<0.05$). There is evidence of transgene recombination and expression of both K-*ras4A* and K-*ras4B* in splenic lymphocytes (Figures 2 and 3), which may explain the increased susceptibility to lymphoma formation. The β-NF-treated K-*ras*^{V12}/*Cre*/*Msh2*$^{-/-}$ test mice mostly succumbed to multiple intestinal tumours (occasionally with associated rectal prolapse), causing bowel obstruction and some also had thymic lymphomas which may have partially contributed to their demise. The increased tumour frequency and reduced survival (Figure 5) indicates that K-*ras*^{V12} expression can cooperate with *Msh2* deficiency to accelerate progression of intestinal tumours as this was associated with a large increase in the number of tumours, particularly in the large intestine as well as in the small intestine.

*Analysis of intestinal tumours for expression of K-*ras^{V12}
To determine the proportion of intestinal tumours in which K-*ras*^{V12} transgene recombination and K-*ras*^{V12} expression occurred following β-NF treatment of K-*ras*^{V12}/*Cre*/*Msh2*$^{-/-}$ mice, LITs of size >3 mm and small intestinal tumours (SITs) were tested for evidence of transgene recombination by PCR and K-*ras*^{V12} transcript and protein expression. Genomic DNA analysis showed *LoxP* recombination in 24 of 27 (88.8%) LITs and 28 of 34 (82.3%) SITs (Figure 6). The intestinal adenomas showing transgene recombination did not differ in terms of size, stage or degree of dysplasia from those tumours not showing transgene recombination. Those tumours with transgene recombination demonstrated expression of K-*ras*^{V12}4A and 4B transcripts by RT–PCR analysis and K-*ras*^{V12} protein expression by Western blot analysis (Figure 6).

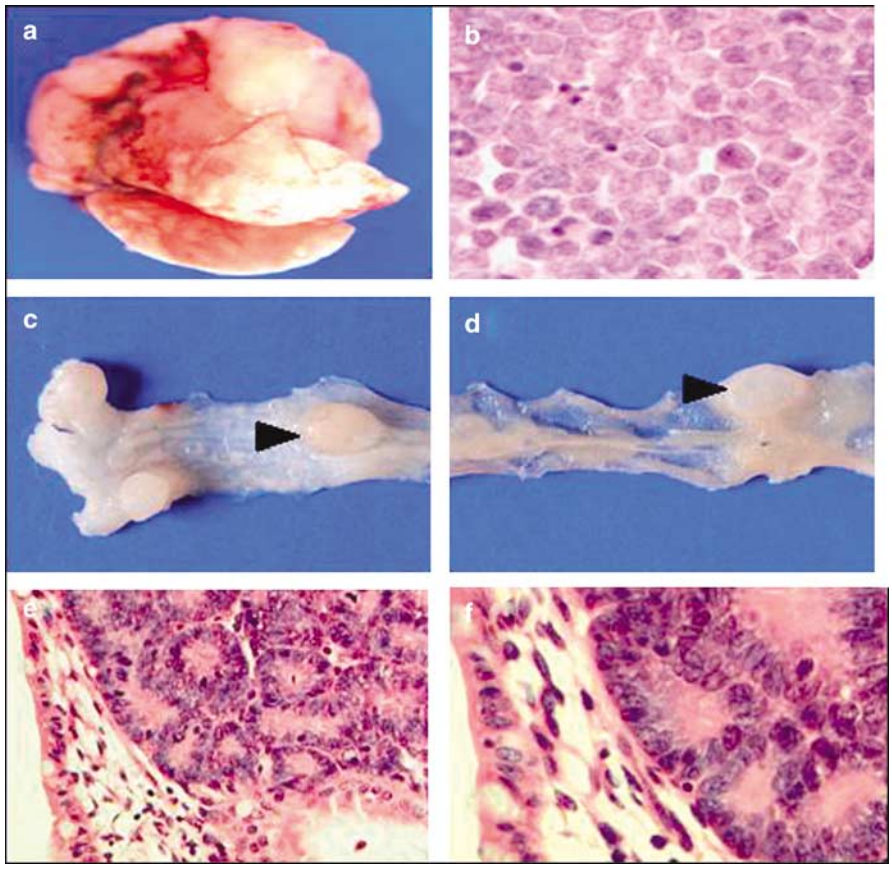

Figure 4 Tumour development in K-*ras*^{V12}/*Cre*/*Msh2*$^{-/-}$ transgenic mice after β-NF treatment. (**a**) Large (4 mm) thymic lymphoma. (**b**) Histological appearances of a diffuse large cell thymic lymphoma (magnification $\times 400$). (**c**) Multiple adenomas in the large intestine (large 3 mm adenoma shown by arrowhead). (**d**) Large adenoma in the small intestine (arrowhead). (**e** and **f**) Histological appearances of a large intestinal adenoma (moderately dysplastic, showing no invasion) with normal intestinal epithelium to the left and bottom of the image (magnification $\times 100$ (**e**) and $\times 400$ (**f**)).

DNA sequencing of the endogenous murine K-*ras* gene showed two of 10 adenomas (three LITs and seven SITs) from *Msh2*$^{-/-}$ mice contained GC→AT transition mutations (at codon 12 of murine K-*ras*), but no mutations in 17 adenomas (five LITs + 12 SITs) from K-*ras*^{V12}/*Cre*/*Msh2*$^{-/-}$ mice. We also sequenced the hot spot mutation region of B-*raf* (exon 15), but found no mutations in any of these same two groups of tumours (data not shown).

*The expression of K-*ras^{V12} *leads to activation MAPK and Akt/PKB pathways*

To investigate whether expression of K-*ras*^{V12} in intestinal tissues and tumours induced functional activation of either or both of the mitogen-activated protein kinase (MAPK) and Akt/protein kinase B (PKB) pathways, which are two of the main downstream signaling pathways for K-*ras*, Western blotting was used to detect presence of the proteins and changes in phosphorylation of a number of MAPK and Akt signaling pathway members. Western blotting showed that p42MAPK and p44MAPK were phosphorylated in large and small intestinal tissues of K-*ras*^{V12}/*Cre* and K-*ras*^{V12}/*Cre*/*Msh2*$^{-/-}$ mice (compared with *Cre* mice) and in a K-*ras*^{V12}/*Cre*/*Msh2*$^{-/-}$ large intestinal adenoma (Figure 7a). Phosphorylated p54JNK and p46JNK were mildly increased in the small intestinal tissue and a large intestinal adenoma. There was a very mild increase in phosphorylated Raf (Ser 259) in a large intestinal adenoma of K-*ras*^{V12}/*Cre*/*Msh2*$^{-/-}$ mice. The Akt/PKB protein expression levels showed no obvious change between transgenic and control mice, but levels of both phosphorylated Akt/PKB and phosphorylated glycogen synthase kinase 3β (GSK-3β) were mildly increased in K-*ras*^{V12}/*Cre* small and large intestinal tissues and moderately increased in K-*ras*^{V12}/*Cre*/*Msh2*$^{-/-}$ LIT tissue (Figure 7a). Results suggest that the expression of K-*ras*^{V12} leads to activation of both MAPK and Akt/PKB signaling pathways.

A previous study showed that when the same mutant K-*ras*^{V12} transgene was introduced into mouse ES cells, the expression of human K-*ras*^{V12} was associated with changes in expression of *Pem*, *Tcl-1* and *Trap1a* gene transcripts, which were increased 2.9-, 7.4- and 4.3-fold, respectively (Luo *et al*., (submitted)). Here, we used RT–qPCR to compare the relative mRNA expression levels of these genes between LITs of β-NF-treated

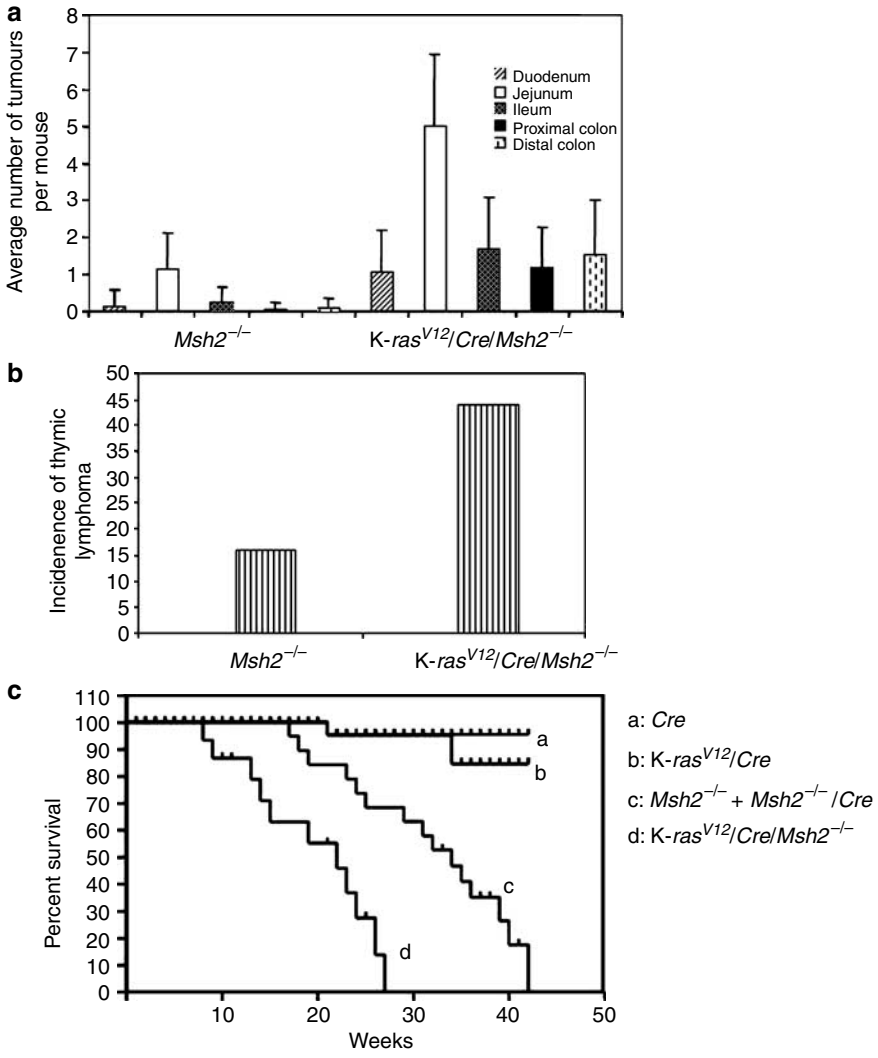

Figure 5 Differences in number and location of tumours and in lifespan for β-NF-treated K-*ras*^{V12}/*Cre*/*Msh2*$^{-/-}$ transgenic mice compared to control mice. (**a**) Numbers of adenomas in the different parts of the gastrointestinal tract of β-NF treated K-*ras*^{V12}/*Cre*/*Msh2*$^{-/-}$ transgenic mice ($n=25$) compared to β-NF-treated *Msh2*$^{-/-}$ control mice ($n=25$) (error bars = s. d.). (**b**) Incidence of thymic lymphomas in the chest of β-NF treated K-*ras*^{V12}/*Cre*/*Msh2*$^{-/-}$ transgenic mice (4/25) compared to β-NF-treated *Msh2*$^{-/-}$ control mice (11/25). (**c**) Kaplan–Meier survival curves for β-NF-treated *Cre* mice ($n=29$), β-NF-treated K-*ras*^{V12}/*Cre* mice ($n=28$), β-NF-treated *Msh2*$^{-/-}$ mice (combined group of 18 *Msh2*$^{-/-}$ mice and 7 *Msh2*$^{-/-}$/*Cre* mice), and β-NF-treated K-*ras*^{V12}/*Cre*/*Msh2*$^{-/-}$ mice ($n=25$). Ages of the animals at death are given in weeks.

K-*ras*^{V12}/*Cre*/*Msh2*$^{-/-}$ mice and normal intestinal tissue of the *Msh2*-deficient control mice to show that expression levels of *Pem*, *Tcl-1* and *Trap1a* gene transcripts were increased by 4.9-, 14.4- and 7.3-fold, respectively, in the LITs known to have recombined and expressed the K-*ras*^{V12} transgene (Figure 7b).

Discussion

Formation of human colorectal neoplasms involves accumulation of genetic and epigenetic changes in a multistep process, including mutational activation of the K-*ras* proto-oncogene, in the stem cells of intestinal crypts (Fearon *et al*., 1987). Several attempts have been made so far to develop murine models of activation of K-*ras* to investigate its role in neoplasia, but these have had only limited success regarding intestinal tumorigenesis (Jackson *et al*., 2001; Meuwissen *et al*., 2001; Guerra *et al*., 2003; Caulin *et al*., 2004; Tuveson *et al*., 2004; Dinulescu *et al*., 2005; Qian *et al*., 2005; Sansom *et al*., 2006). Transgenic expression of mutated K-*ras* in the small intestine in villus enterocytes under the control of the rat liver fatty acid binding protein gene (*Fabp1*) promoter caused no tumours, and concern was expressed relating to the lack of expression in stem cells and the short residence time of migrating enterocytes on the villus with exfoliation every 2 to 3 days, possibly allowing insufficient time for accumulation of other genetic mutations (Kim *et al*., 1993; Janssen *et al*., 2002, 2005). Transgenic expression of mutated K-*ras* by the villin promoter has been reported in intestinal stem cells, and these mice have been shown to develop intestinal

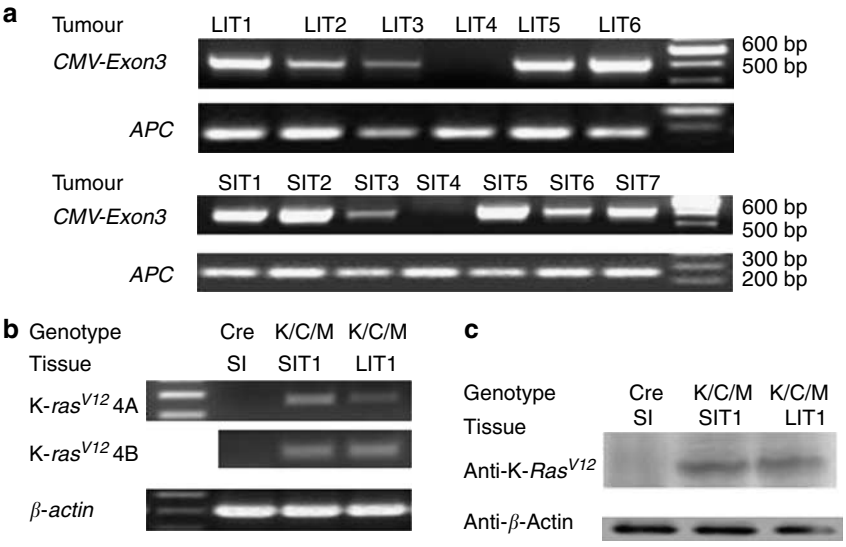

Figure 6 Transgene recombination and expression of K-ras^{V12} in intestinal adenomas. (**a**) Transgene recombination assay with PCR amplification of genomic DNA using primers located in the *CMV* promoter and K-ras^{V12} exon 3, generated a ~500 bp fragment from recombined sequences in adenomas from the small and large intestines, only if Cre-mediated recombination at the *LoxP* sites had occurred in the K-ras^{V12} transgene. LIT1 to LIT9, large intestinal tumours; SIT1 to SIT8, small intestinal tumours. Amplification of a DNA fragment of the APC gene was used as a control for adequate quality of genomic DNA. (**b**) RT–PCR analysis of the expression of K-ras^{V12} 4A and 4B transcript isoforms in selected (recombination-positive) small and large intestinal adenomas of β-NF-treated K-ras^{V12}/*Cre*/$Msh2^{-/-}$ transgenic mice. K/C/M, K-ras^{V12}/*Cre*/$Msh2^{-/-}$ mice; 4A, 4A transcript of K-ras^{V12}; 4B, 4B transcript of K-ras^{V12}. RT–PCR amplification of a β-actin transcript fragment was used to control the quality of RNA samples. (**c**) Western blot analysis of the expression of mutant K-Ras protein using anti-K-Ras^{V12} protein antibody in selected small and large intestinal adenomas of β-NF-treated K-ras^{V12}/*Cre*/$Msh2^{-/-}$ transgenic mice.

tumours (Janssen *et al*., 2002). K-*ras* mutation-prone latent alleles (with activation occurring by recombination within the latent allele in random cells) were highly predisposed to a range of tumour types, predominantly early onset lung cancer, but although aberrant crypt foci occurred the transgenic mice failed to develop intestinal tumours, perhaps owing to tissue-specific differences in the frequency of recombination events, or other factors (Johnson *et al*., 2001; Meuwissen *et al*., 2001). Hence, we set out to design and characterize an *in vivo* model system with inducible expression of mutated K-*ras* in the stem cells of the intestinal crypt epithelium, using a *Cre*/*LoxP* system.

We generated a transgenic line of mice with a single integrated copy of a K-ras^{V12} transgene capable of being activated by Cre-mediated recombination at two *LoxP* sites that spanned a 'STOP' sequence preventing transgene expression in non-recombined cells. This was crossed with mice bearing an *Ah-Cre* transgene, demonstrated previously to show β-naphthoflavone-induced intestinal expression of *Cre* that mediates *LoxP* recombination in adult intestinal epithelial stem cells of both small and large intestines (Ireland *et al*., 2004). The test offspring containing both transgenes were used to investigate the effects of mutated K-*ras* expression in the intestines upon the initiation or early events in intestinal tumorigenesis *in vivo*. In contrast to other previous studies, this work introduced a human mutated K-*ras* 'minigene' capable of expression of both K-*ras* 4A and K-*ras* 4B isoforms, as it contains both exons 4A and 4B of the K-*ras* gene, which has previously been shown to induce more efficient transformation of cells grown in culture (Capon *et al*., 1983). The human K-*ras* protein amino-acid sequence is very highly homologous to that of the mouse. After treating with β-NF, we confirmed intestinal epithelial expression of *Cre* protein and *LoxP* recombination by PCR and DNA sequencing. We demonstrated expression of K-ras^{V12} transcripts (both 4A and 4B) and protein by RT–PCR and Western blot analysis in the small and large intestines and some other tissues. After such induction by β-NF, we detected only a minimal phenotypic change in the intestines of K-ras^{V12}/*Cre* mice with just two tumours in the intestines (one adenoma in the large intestine and one adenoma in the small intestine in 20 mice over nearly 2 years (another eight mice were killed after 1 year and showed no intestinal tumours). The appearance of only a very few tumours, consistent with previous studies (Janssen *et al*., 2002), and no tumours in other tissues, may reflect the possibility that expression of mutated K-*ras* in intestinal epithelium may be largely unable to initiate intestinal tumour formation on its own, as it appears to be dependent on cellular context (Guerra *et al*., 2003) and may need other, possibly multiple, mutations in other genes in the epithelium, and this is consistent with mutated K-*ras* initiation of intestinal tumorigenesis being a rare or negligible event.

Defective DNA MMR is associated with a markedly increased mutation rate and with initiation and/or acceleration of neoplasia in the intestines and elsewhere, as seen in HNPCC and its *Msh2*-deficient murine model (de Wind *et al*., 1995; Reitmair *et al*., 1995, 1996; Toft

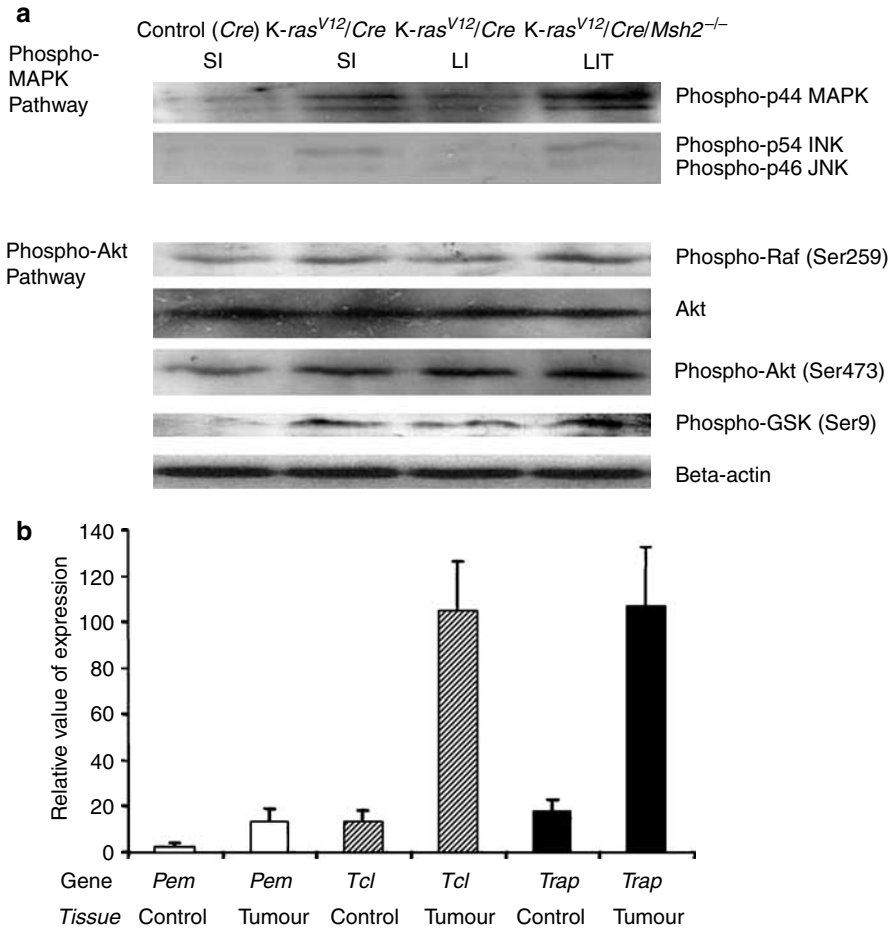

Figure 7 The expression of K-ras^{V12} leads to activation by phosphorylation of MAPK and Akt/PKB pathway downstream proteins. (**a**) Western blotting analysis showed p42MAPK and p44MAPK were phosphorylated in large and small intestinal tissues of K-ras^{V12}/*Cre* mice and in a LIT of K-ras^{V12}/*Cre*/$Msh2^{-/-}$ mice. Phosphorylated p54JNK and p46JNK were mildly increased in the small intestinal tissues of K-ras^{V12}/*Cre* mice and in a LIT of K-ras^{V12}/*Cre*/$Msh2^{-/-}$ mice. There was a mild increase in phosphorylated Raf (Ser 259) in a large intestinal adenoma of K-ras^{V12}/*Cre*/$Msh2^{-/-}$ mice. The expression levels of Akt/PKB protein showed no obvious difference between test and control tissues or tumours, but both phosphorylated Akt/PKB (Ser 473) and phosphorylated glycogen synthase kinase 3β (GSK Ser 9) showed a mild increase in small and large intestinal tissues of K-ras^{V12}/*Cre* mice and a moderate increase in a large intestinal adenoma of K-ras^{V12}/*Cre*/$Msh2^{-/-}$ mice. (**b**) RT–qPCR analysis of the expression of *Pem*, *Tcl-1* and *Trap1a* genes in three large intestinal adenomas from β-NF treated K-ras^{V12}/*Cre*/$Msh2^{-/-}$ transgenic mice compared to normal large intestinal tissue from $Msh2^{-/-}$ mice.

and Arends, 1998; Toft *et al*., 1999, 2002; Frayling *et al*., 2005). *Msh2*-deficient mice are predisposed to develop gastrointestinal tumours, thymic lymphomas and some tumours of other organ systems, and although some of the *Msh2*-deficient mice develop colonic adenomatous polyps, most tumours of the gastrointestinal tract are predominantly found in the small intestine (de Wind *et al*., 1995, 1998; Toft *et al*., 1999). To study the role of mutant K-ras^{V12} in MMR-deficient intestinal tumour development and progression *in vivo*, we crossed the K-ras^{V12}/*Cre* double transgenic mice with $Msh2^{-/-}$ mice to allow conditional activation of the K-ras^{V12} transgene in the intestines on an MMR-deficient background. The β-NF-treated K-ras^{V12}/$Msh2^{-/-}$/*Cre* test mice showed a 20-fold increase in large intestinal adenomas ($P<0.01$) and a fivefold increase in small intestinal adenomas ($P<0.01$) compared to control $Msh2^{-/-}$ mice. Over 80% of intestinal tumours from these mice showed K-ras^{V12} transgene recombination and expression of K-ras^{V12} transcripts and proteins, including 82% of SITs and 89% of large intestinal tumours, the remainder appear to have developed as $Msh2^{-/-}$-mediated tumours (without K-ras^{V12} expression) as seen in the $Msh2^{-/-}$ control mice, most probably reflecting the random spatial pattern within the intestines of β-NF-induced *Cre*-mediated *LoxP* recombination (Ireland *et al*., 2004). Endogenous murine K-*ras* gene mutations were found in 20% of control $Msh2^{-/-}$ mouse adenomas but in none of the adenomas from the K-ras^{V12}/*Cre*/$Msh2^{-/-}$ test mice and there were no mutations in the mutational hot spot in exon 15 of B-*raf*. The K-ras^{V12}/*Cre*/$Msh2^{-/-}$ test mice showed statistically significantly reduced survival from 27 to 17 weeks, compared with both $Msh2^{-/-}$ and *Cre*-only controls and with K-ras^{V12}/*Cre* controls (with

identical β-NF treatments to all groups). Thus, K-*ras*^{V12} expression cooperates synergistically with *Msh2* deficiency *in vivo* to accelerate progression of intestinal adenomas.

The effect of mutated K-*ras* on increased progression, but not initiation, of adenoma development was greater in the large intestine relative to the small intestine. Expression of mutated K-*ras* transcripts (4A and 4B) and proteins in those intestinal tumours showing *LoxP* recombination was confirmed by RT–PCR and Western blot analysis. Expression of K-*ras*^{V12} in intestinal tissues and tumours induced functional activation of both of the MAPK and Akt/PKB pathways, with evidence of phosphorylation of p42MAPK, p44MAPK, p54JNK, p46JNK, Raf, Akt/PKB and GSK-3β. Further evidence of the functional effects of K-*ras*^{V12} expression was shown by the demonstration in these tumours of increased expression of *Pem*, *Tcl-1* and *Trap1a*, which are genes implicated in tumour development and growth that we have shown previously to be increased in expression in ES cells following activation of expression of K-*ras*^{V12} (Luo *et al*.). However, the precise molecular mechanisms by which mutated K-*ras* and MMR deficiency interact *in vivo* to accelerate intestinal tumorigenesis require further study.

Materials and methods

*Construction of the conditional K-*ras^{V12} *expressing transgene*
The conditional K-*ras*^{V12} expression transgene construct was generated as follows. The human K-*ras*^{V12} 'minigene' was derived from plasmid set II K-*ras*^{V12} 'minigene' (Capon *et al*., 1983; Brooks *et al*., 2001), which contains exons 1, 2, 3, 4A and 4B, together with introns between exons 3, 4A and 4B, such that this K-*ras*^{V12} 'minigene' is capable of expressing both K-ras 4A and 4B transcripts. The second *Bam*H1 site in the middle of the K-*ras*^{V12} 'minigene' was destroyed by partial digestion and re-ligation before cloning and the *Eco*RI–*Bam*HI fragment containing the K-*ras*^{V12} 'minigene' was cloned into the pBluescript II KS plasmid with a *CMV* promoter sequence and *NotI* site upstream of it. Into the *Not*I restriction enzyme site of this plasmid, between the *CMV* promoter and the K-*ras*^{V12} 'minigene', a multi-enzyme linker DNA oligonucleotide containing restriction enzyme recognition sites and two *Lox*P sites was inserted: *Not*I–*Lox*P–*Hind*III–*Xho*I–*Lox*P–*Not*I (5′GGCCGCATAACTTCGTATAGCATACATTATACGAAGTTATAAGCTTATTTGAGGCTCGAGAAATAACTTCGTATAGCATACATTATACGAAGTTATAGCTGGC3′). After digestion with *Hind*III and *Xho*I, a 'STOP' cassette element containing a neomycin resistance gene (*Neo*) was inserted into the *Hind*III and *Xho*I enzyme site overhangs. This plasmid was subsequently digested by HindIII and re-ligated in order to excise the *Hind*III–*PKG*–*Hind*III fragment in the construct. Finally, downstream of the K-*ras*^{V12} 'minigene' a DNA sequence containing an IRES and a gene encoding EGFP was inserted, to generate the final K-*ras*^{V12} transgene construct (Figure 1). The construct was linearized using *Bam*HI, purified by agarose gel electrophoresis with electro-elution, and micro-injected into fertilized FVB/N mouse oocytes to generate founder mice.

*PCR-based genotyping of K-*ras^{V12} *mice*
For genotyping, four pairs of primers for PCR assays were developed for rapid screening of K-*ras*^{V12} positive mice (Figure 1). The quality of tail genomic DNA was estimated by amplifying a wild-type APC gene fragment. PCR conditions were 95.0°C for 30 s, 60.0°C for 30 s and 72.0°C for 45 s for 35 cycles. The sequences of PCR primers were as follows: *EGFP* sense, 5′GCAAGGGCGAGGAGCTGTTC3′; *EGFP* antisense, 5′CCATGCCGAGAGTGATCCCG3′; human mutated K-*ras* 4B sense, 5′TCTTAAGGCATACTAGTACAAGTGGT3′; human mutated K-*ras* 4B antisense, 5′TTTGTTTCACACCAACATTCA3′; *CMV* promoter sense, 5′TGACGTCAATGGGTGGAGTA3′; *CMV* promoter antisense, 5′TGCCAAAACAAACTCCCATT3′; *Neo* sense, 5′TGGAGAGGCTATTCGGCTATGACTGGG3′; *Neo* antisense, 5′TGGATACTTTCTCGGCAGGAGCAAGGTG3′; *Apc* sense, 5′TGATACTTCTTCCAAAGCTTTGGCTAT3′; *Apc* antisense, 5′TCTCGTTCTGAGAAAGACA GAAGCT3′.

*RT–qPCR was used to identify the copy number of the K-*ras^{V12} *transgene*
To estimate how many copies of human K-*ras*^{V12} transgene were integrated into the mouse genome, RT–qPCR was used to amplify K-*ras* sequences from both endogenous murine K-*ras* proto-oncogene and the integrated human K-*ras*^{V12} transgene. We designed one pair of primers that bound with identical specificity to both human and mouse K-*ras* exon 3 sequences: K-*ras* mouse/human exon 3 sense, 5′TTATTGATGGAGAAACCTGTCTCTTG3′, K-*ras* mouse/human exon 3 antisense, 5′TTATGGCAAATACACAAAGAAAGCC3′. Briefly, 100 ng DNA from control C57B6/J(*B6*) and from mice containing the K-*ras*^{V12} transgene was used for RT–qPCR, using the iCycler (BioRad, Hercules, CA, USA) starting with denaturation at 95.0°C for 3 min, then 35 cycles of 95.0°C for 15 s and 60.0°C for 1 min. All PCR products were quantitatively analysed in the linear range of the log-plotted exponential phase of PCR amplification. The quantity of the specific K-*ras*-derived fragments was obtained from standard curves with normalization using the wild-type *Apc* gene by PCR of the same sample (performed in triplicate).

*Generation of K-*ras^{V12}/Cre *mice and* Msh2*-deficient K-*ras^{V12}/Cre *mice*
K-*ras*^{V12} transgene containing mice (on a *FVB/N* background) were crossed five to seven times with *B6* mice, so the K-*ras*^{V12} transgene was mainly on B6 background (more than 31/32 proportionally of B6 and less than 1/32 of FVB/N genetic background). These *K-ras*^{V12} mice were crossed with *Ah-Cre* mice, which allow transient intestinal expression of *Cre* protein, that can mediate recombination of the K-*ras*^{V12} transgene, following injection of β-naphthoflavone (β-NF) via the *Ah* promoter (Ireland *et al*., 2004). Subsequently, the *K-ras*^{V12}/*Cre* mice were crossed with *Msh2*$^{-/-}$ mice to generate *K-ras*^{V12}/*Cre*/*Msh2*$^{-/-}$ triple mutant mice. The mice were genotyped for *Msh2* status and for *Cre* status by PCR assays (Toft *et al*., 1999; Ireland *et al*., 2004).

β-*NF-induced expression of Cre and subsequent expression of K-*ras^{V12}
In order to induce Cre expression via the Ah promoter, mice were injected with 16 mg/kg β-NF (Sigma, Dorset, UK) dissolved in warm corn oil, for 6 days (Ireland *et al*., 2004). Human K-*ras* 4A and K-*ras* 4B expression was determined using human DNA sequence-specific PCR primer pairs: K-*ras* 4A sense, 5′AGTGCAATGAGGGACCAGTACATGAGG3′ located in K-*ras* exon 3; and K-*ras* 4A antisense, 5′TTTGCTGATGTTTCAATAAAAGGAATT3′ located in K-*ras* exon 4A; K-*ras* 4B sense, 5′GTACCTATGGTCCTAGTAGGAAATAAA3′ also located in human K-*ras* exon 3; and

K-*ras* 4B antisense, 5′CTGATGTTTCAATAAAGGAATT CCA3′ located in human K-*ras* exon 4B. The PCR product sizes for human K-*ras* 4A and 4B were 267 and 188 bp, respectively. For RT–qPCR, 100 ng of total RNA of different tissue samples was reverse transcribed in 25 ml volume using the iTaq SYBR Green kit RT–PCR kit (Bio-RAD). All PCR reactions were amplified starting with denaturation at 95°C for 3 min, then 45 cycles of 95°C for 15 s and 60°C for 1 min. The specificity of the PCR reactions was determined by 2% agarose gel electrophoresis and PCR of *β-actin* as quality control of all samples.

PCR analysis of transgene LoxP *site recombination and DNA sequencing*

Genomic DNA was prepared from intestinal tumours and non-tumour gastrointestinal tissue and other tissue samples. The PCR primers used to identify recombination between the *CMV* promoter and the K-*ras* transgene were as follows: RE-*CMV* sense, 5′TCAGATCACTAGAAGCTTTATTGCGG3′, which is located in the *CMV* promoter; and RE-K-*ras* antisense, 5′TTCTGAATTAGCTGTATCGTCAAGGC3′, which is located in exon 3 of the human K-*ras*^{V12} transgene. This PCR assay can detect recombination of the two *Lox*P sites. The same PCR primers were used as DNA sequencing primers to sequence the PCR product from both termini by standard methods.

Western blot analysis of Ras and Cre protein expression

Fresh tissue samples were lysed in protein lysis buffer (50 mM Tris-HCl, pH 7.4, 150 mM NaCl, 0.5% NP-40) and protease inhibitors were added. Extracts were separated by 15% sodium dodecyl sulphate–polyacrylamide gel electrophoresis, transferred to nitrocellulose filters, and incubated with the corresponding antibodies including anti-pan-K-Ras and anti-K-Ras^{V12} antibodies (Oncogene Co., Cambridge, MA, USA) and anti-Cre rabbit polyclonal antibody (Novagen, San Diego, CA, USA) (all antibodies were used at 1:1000 dilution). The Phospho-Akt Pathway Sampler kit and the phospho-MAPK Family Antibody Sampler kit (Cell Signaling Technology, Beverly, MA, USA) were used for Western blot analysis of the Akt and MAPK pathway proteins (phospho-p44MAPK, phospho-p38MAPK, phospho-p54JNK, phospho-p46JNK, phospho-Raf (Ser259), Akt, phospho-Akt (Ser473) and Phospho-GSK3beta (Ser9)) according to the manufacturer's protocol. Antibodies were detected with the appropriate goat or rabbit peroxidase-linked secondary antibody and visualization with the NBT/BCIP kit following the manufacturer's instructions (Roche Co, Indianapolis, IN, USA).

Analysis of intestinal tumours

Mice that developed tumours died or were killed when moribund due to tumour burden (mostly due to multiple intestinal tumours, with or without thymic lymphomas). The small and large intestines were carefully dissected. The whole intestinal tract of each mouse was removed, rinsed gently in phosphate-buffered saline using a syringe and opened lengthwise. The opened intestine was spread flat on filter paper, and fixed in 10% neutral-buffered formalin solution. The numbers of intestinal polyps were counted under a dissecting microscope at $\times 15$ magnification, always by the same investigator. The smallest adenomatous polyps identified were about 0.5–1.0 mm in diameter. Tumours of the small and large intestines and other tissues were processed for paraffin embedding. Sections were prepared for haematoxylin and eosin staining and histological examination for identification of tumour type and stage.

RT–qPCR was used to assess gene expression in intestinal tumours

RT–qPCR was carried out to measure the relative levels of *Pem*, *Tcl-1* and *Trap1a* gene expression using the comparative C_t method as previously described (Al-Aynati *et al*., 2004; Zhu *et al*., 2004; Luo *et al*., submitted). The values for *β-actin* were used to normalize the gene expression data. The gene expression levels in tumour cells relative to the control group intestinal tissues (from the *Msh2*$^{-/-}$ group) were calculated using the following formulas: $\Delta\Delta C_t = \Delta C_t$ test $- \Delta C_t$ control, fold change $= 2^{-\Delta\Delta Ct}$. PCR primers: *β-actin*, sense, 5′AAGC TGTGCTATGTTGCTCTAGACT3′ and *β-actin* antisense, 5′CACTTCATGATGGAATTGAATGTAG3′; *Pem*, sense, 5′GAGTCAAG GAAGACTCGGAAGA3′ and *Pem* antisense, 5′GGCCTTTTCCTCCATTTAATTC3′; *Tcl-1* sense, 5′CAAGAGTAATGAAAAATTCCAGGTG3′ and *Tcl-1* antisense, 5′GATATGGTACAGGATCTGCCAATAC3′; and *Trap1a*, sense, 5′AAGAATTGGAGAACCTGATGGA3′ and *Trap1a* antisense, 5′GGGTCGTGG AAGAAATAAATCA3′.

DNA sequencing

Parts of the adenoma tissue were cut from SITs or LITs and DNA was extracted. PCR was used to amplify sequences of endogenous murine K-*ras* exons 1, 2 and 3. PCR primers were used as the DNA sequencing primers to sequence the samples by standard methods. The sequences of PCR primers were as follows: mouse K-*ras* exon 1, sense, 5′CGTCCTTTAC AAGCGCACGCAGACT3′, antisense, 5′CCATGTATTTTA TTAAGTGTTGATGA3′; mouse K-*ras* exon 2, sense, 5′AG ATCATGCAGGCATAACAATTAG3′, antisense, 5′CTGTT TTGAATGGGGTCTTCTATT3′; mouse K-*ras* exon 3, sense, 5′GAAATGAAGATCAATGACGAACAC3′, antisense, 5′GT GAAGACAATTTGGTAGGGTAGAA3′; and mouse B-*raf* exon 15, sense, 5′GGCTTACAATGTTATTCCTGTGAGT3′, antisense, 5′TTTTACCTGAAATCTTCAAAATGCT3′.

Statistical analysis

Statistical analysis was by Student's *t*-test for comparisons of test and control groups and by log-rank test for comparison of the Kaplan–Meier survival curves. A $P < 0.05$ was taken to be statistically significant.

Acknowledgements

We thank Clive Lebozer and Xinping Gong (Department of Pathology, University of Cambridge) for technical assistance. This work was supported by grants from Cancer Research UK and the Wellcome Trust.

References

Al-Aynati MM, Radulovich N, Riddell RH, Tsao MS. (2004). Epithelial-cadherin and beta-catenin expression changes in pancreatic intraepithelial neoplasia. *Clin Cancer Res* **10**: 1235–1240.

Andreyev HJ, Norman AR, Cunningham D, Oates J, Dix BR, Iacopetta BJ *et al*. (2001). Kirsten ras mutation in patients with colorectal cancer: the 'RASCAL II' study. *Br J Cancer* **85**: 692–696.

Arends MJ, Frayling I. (2004). The genetics of colorectal cancer: mismatch repair deficiency in hereditary and sporadic colorectal cancer. In: Cunningham D, Topham C, Miles A (eds). *Key Advances in the Effective Management of Colorectal Cancer* Chapter 2, 4th edn., Aesculapius Medical Press: London, pp 25–40.

Arends MJ, McGregor AH, Toft NJ, Brown EJ, Wyllie AH. (1993). Susceptibility to apoptosis is differentially regulated by c-myc and mutated Ha-*ras* oncogenes and is associated with endonuclease availability. *Br J Cancer* **68**: 1127–1133.

Arends MJ, McGregor AH, Wyllie AH. (1994). Apoptosis is inversely related to necrosis and determines net growth in tumours bearing constitutively expressed myc, ras, and HPV oncogenes. *Am J Pathol* **144**: 1045–1057.

Barbacid M. (1987). Ras genes. *Annu Rev Biochem* **56**: 779–827.

Brooks DG, James RM, Patek CE, Williamson J, Arends MJ. (2001). Mutant K-ras enhances apoptosis in embryonic stem cells in combination with DNA damage and is associated with increased levels of p19 (ARF). *Oncogene* **20**: 2144–2152.

Capon DJ, Seebrug PH, McGrath JP, Hayflick JS, Edman U, Levinson AD *et al*. (1983). Activation of Ki-ras2 gene in human colon and lung carcinomas by two different point mutations. *Nature* **304**: 507–513.

Caulin C, Nguyen T, Longley MA, Zhou Z, Wang XJ, Roop DR. (2004). Inducible activation of oncogenic K-ras results in tumour formation in the oral cavity. *Cancer Res* **64**: 5054–5058.

de Wind N, Dekker M, Berns A, Radman M, te Riele H. (1995). Inactivation of the mouse Msh2 gene results in mismatch repair deficiency, methylation tolerance, hyperrecombination, and predisposition to cancer. *Cell* **82**: 321–330.

de Wind N, Dekker M, van Rossum A, van der Valk M, te Riele H. (1998). Mouse models for hereditary nonpolyposis colorectal cancer. *Cancer Res* **58**: 248–255.

Dinulescu DM, Ince TA, Quade BJ, Shafer SA, Crowley D, Jacks T. (2005). Role of K-ras and Pten in the development of mouse models of endometriosis and endometrioid ovarian cancer. *Nat Med* **11**: 63–70.

Fearon ER, Hamilton SR, Vogelstein B. (1987). Clonal analysis of human colorectal tumours. *Science* **238**: 193–197.

Frayling IM, Happerfield L, Mattocks C, Oakhill K, Arends MJ. (2005). Application of molecular diagnostics to hereditary nonpolyposis colorectal cancer (Chapter 32). In: Coleman WB, Tsongalis GJ (eds). *Molecular Diagnostics, For the Clinical Laboratorian* 2nd edn. Humana Press Inc: NJ, pp 375–392.

Guerra C, Mijimolle N, Dhawahir A, Dubus P, Barradas M, Serrano M *et al*. (2003). Tumour induction by an endogenous K-ras oncogene is highly dependent on cellular context. *Cancer Cell* **4**: 111–120.

Ireland H, Kemp R, Houghton C, Howard L, Clark AR, Sansom OJ *et al*. (2004). Inducible Cre-mediated control of gene expression in the murine gastrointestinal tract: effect of loss of β-catenin. *Gastroenterology* **126**: 1236–1246.

Jackson EL, Willis N, Mercer K, Bronson RT, Crowley D, Montoya R *et al*. (2001). Analysis of lung tumour initiation and progression using conditional expression of oncogenic K-ras. *Genes Dev* **15**: 3243–3248.

James RM, Arends MJ, Plowman S, Brooks DG, Miles CG, West JD *et al*. (2003). K-ras proto-oncogene exhibits tumour suppressor activity as its absence promotes tumorigenesis in murine teratomas. *Mol Cancer Res* **1**: 820–825.

Janssen KP, Abala M, EI Marjou F, Louvard D, Robine S. (2005). Models of K-ras-initiated carcinogenesis. *Biochim Biophys Acta* **1756**: 145–154.

Janssen KP, Marjou FE, Pinto D, Sastre X, Rouillard D, Fouquet C *et al*. (2002). Targeted expression of oncogenic K-ras in intestinal epithelium cause spontaneous tumourigenesis in mice. *Gastroenterology* **123**: 492–504.

Jiricny J, Nystrom-Lahti M. (2000). Mismatch repair defects in cancer. *Curr Opin Genet Dev* **10**: 157–161.

Johnson L, Mercer K, Greenbaum D, Bronson RT, Crowley D, Tuveson DA *et al*. (2001). Somatic activation of the K-ras oncogene causes early onset lung cancer in mice. *Nature* **410**: 1111–1116.

Kim SH, Roth KA, Moser AR, Gordon JI. (1993). Transgenic mouse models that explore the multistep hypothesis of intestinal neoplasia. *J Cell Biol* **123**: 877–893.

Kinzler KW, Vogelstein B. (1996). Lessons from hereditary colorectal cancer. *Cell* **87**: 159–170.

Luo F, Hamoudi R, Brooks DG, Patek CE, Arends MJ. (2007). Microarray profiling of changes in gene expression induced by K-ras^{Val12} in embryonic stem cells. (Submitted Manuscript to BMC Genomics).

Malumbres M, Barbacid M. (2003). RAS oncogenes: the first 30 years. *Nat Rev Cancer* **3**: 459–465.

Meuwissen R, Linn SC, van der Valk M, Mooi WJ, Berns A. (2001). Mouse model for lung tumorigenesis through Cre/lox controlled sporadic activation of the K-Ras oncogene. *Oncogene* **20**: 6551–6558.

Morris RG, Curtis LJ, Romanowski P, Hardcastle JD, Jenkins DA, Robinson M *et al*. (1996). Ki-ras mutations in adenomas: a characteristic of cancer-bearing colorectal mucosa. *J Pathol* **180**: 357–363.

Otori K, Oda Y, Sugiyama K, Hasebe T, Mukai K, Fujii T *et al*. (1997). High frequency of K-ras mutations in human colorectal hyperplastic polyps. *Gut* **40**: 660–663.

Plowman SJ, Arends MJ, Brownstein DG, Luo F, Devenney PS, Rose L *et al*. (2006a). The K-Ras 4A isoforms promotes apoptosis but does not affect either lifespan or spontaneous tumour incidence in ageing mice. *Exp Cell Res* **312**: 16–26.

Plowman SJ, Berry RL, Bader SA, Luo F, Arends MJ, Harrison DJ *et al*. (2006b). K-ras 4A and 4B are co-expressed widely in human tissues, and their ratio is altered in some sporadic colorectal cancers. *J Exp Clin Cancer Res* **25**: 259–267.

Plowman SJ, Williamson DJ, O'Sullivan MJ, Doig J, Ritchie A-M, Harrison DJ *et al*. (2003). While K-ras is essential for mouse development, expression of the K-ras 4A splice variant is dispensable. *Mol Cell Biol* **23**: 9245–9250.

Qian J, Niu J, Li M, Chiao PJ, Tsao MS. (2005). *In vitro* modeling of human pancreatic duct epithelial cell transformation defines gene expression changes induced by K-ras oncogenic activation in pancreatic carcinogenesis. *Cancer Res* **65**: 5045–5053.

Reitmair AH, Redston M, Cai JC, Chuang TC, Bjerknes M, Cheng H *et al*. (1996). Spontaneous intestinal carcinomas and skin neoplasms in Msh2-deficient mice. *Cancer Res* **56**: 3842–3849.

Reitmair AH, Schmits R, Ewel A, Bapat B, Redston M, Mitri A *et al*. (1995). MSH2 deficient mice are viable and susceptible to lymphoid tumours. *Nat Genet* **11**: 64–70.

Sansom OJ, Meniel V, Wilkins JA, Cole AM, Oien KA, Marsh V *et al*. (2006). Loss of Apc allows phenotypic manifestation of the transforming properties of an endogenous K-ras oncogene *in vivo*. *Proc Natl Acad Sci (USA)* **103**: 14122–14127.

Shivapurkar N, Huang L, Ruggeri B, Swalsky PA, Bakker A, Finkelstein S *et al*. (1997). K-ras and p53 mutations in aberrant crypt foci and colonic tumours from colon cancer patients. *Cancer Lett* **115**: 39–46.

Spandidos DA, Wilkie NM. (1984). Malignant transformation of early passage rodent cells by a single mutated human oncogene. *Nature* **310**: 469–475.

Toft NJ, Arends MJ. (1998). DNA mismatch repair and colorectal cancer. *J Pathol* **185**: 123–129.

Toft NJ, Curtis LJ, Sansom OJ, Leitch AL, Wyllie AH, Te Riele H *et al*. (2002). Heterozygosity for p53 promotes microsatellite instability and tumorigenesis on a Msh2 deficient background. *Oncogene* **21**: 6299–6306.

Toft NJ, Winton DJ, Kelly J, Howard LA, Dekker M, te Riele H *et al*. (1999). Msh2 status modulates both apoptosis and mutation frequency in the murine small intestine. *Proc Natl Acad Sci (USA)* **96**: 3911–3915.

Tuveson DA, Shaw AT, Willis NA, Silver DP, Jackson EL, Chang S *et al*. (2004). Endogenous oncogenic K-ras (G12D) stimulates proliferation and widespread neoplastic and developmental defects. *Cancer Cell* **5**: 375–387.

Yamada S, Yashiro M, Maeda K, Nishiguchi Y, Hirakawa K. (2005). A novel high-specificity approach for colorectal neoplasia: detection of K-ras2 oncogene mutation in normal mucosa. *Int J Cancer* **113**: 1015–1021.

Zhu CQ, Blackhall FH, Pintilie M, Iyengar P, Liu N, Ho J *et al*. (2004). Skp2 gene copy number aberrations are common in non-small cell lung carcinoma, and its over-expression in tumours with ras mutation is a poor prognostic marker. *Clin Cancer Res* **10**: 1984–1991.